Title
QUADRUPOLE MOMENTS OF THE FIRST EXCITED STATES IN 20Ne AND 22Ne

Authors
Nakai, K.
Stephens, F.S.
Diamond, R.M.

Publication Date
1969-12-01

Submitted to Nuclear Physics

UCRL-18959
Preprint

QUADRUPOLE MOMENTS OF THE FIRST EXCITED STATES IN ^{20}Ne AND ^{22}Ne

K. Nakai, F. S. Stephens and R. M. Diamond

December 1969

AEC Contract No. W-7405-eng-48

DISCLAIMER

KEY WORDS

COULOMB EXCITATION: $^{20,22}Ne(^{120}Sn, ^{120}Sn)$ $^{20,22}Ne(^{130}Te, ^{130}Te)$, $^{20,22}Ne(^{148}Sm, ^{148}Sm)$; measured $(d\sigma^{160°}_{projectile}/d\sigma^{160°}_{target})$, $(d\sigma^{90°}_{projectile}/d\sigma^{90°}_{target})$; deduced $Q(^{20}Ne, 2^+)$, $B(E2, ^{20}Ne\ 0^+ \rightarrow 2^+)$, $Q(^{22}Ne, 2^+)$, $B(E2, ^{22}Ne, 0^+ \rightarrow 2^+)$.

QUADRUPOLE MOMENTS OF THE FIRST EXCITED STATES IN ^{20}Ne AND ^{22}Ne[†]

K. Nakai,[††] F. S. Stephens and R. M. Diamond

Lawrence Radiation Laboratory
University of California
Berkeley, California 94720

December 1969

Abstract

Static quadrupole moments of the first excited states of ^{20}Ne and ^{22}Ne have been measured using the reorientation effect in projectile excitation. The Ne nuclei, accelerated by the Berkeley Hilac, were Coulomb excited by thin targets of ^{120}Sn, ^{130}Te or ^{148}Sm and the gamma-ray yields in coincidence with particles scattered at angles of 90° and 160° were evaluated using the deBoer-Winther Coulomb excitation program. The results obtained are $Q(^{20}\text{Ne},2^+) = -0.24 \pm 0.03$ b, $B(E2,^{20}\text{Ne},0^+\rightarrow 2^+) = 0.048 \pm 0.007\ e^2b^2$, $Q(^{22}\text{Ne},2^+) = -0.21 \pm 0.04$ b, and $B(E2,^{22}\text{Ne},0^+\rightarrow 2^+) = 0.033 \pm 0.006\ e^2b^2$.

1. Introduction

The reorientation effect in projectile Coulomb excitation provides a method for determining the quadrupole moment of the first excited state in a number of nuclei. One of the most interesting nuclei to which this method can be applied is ^{20}Ne since it appears to be one of the best examples of a deformed nucleus in the light mass region.

[†]Work performed under the auspices of the U. S. Atomic Energy Commission.

[††]On leave from Osaka University, Toyonaka, Osaka, Japan.

The main advantage of using projectile excitation in a reorientation experiment is that one can expect a larger effect than in the usual target-excitation method. This is because the nuclei of interest are excited by higher Z elements - up to Z = 92. In the usual reorientation experiment, the effect is small ($\sim$ 10%), so that many kinds of corrections and uncertainties are of comparable size and make the interpretation difficult[1]). In the case of ^{20}Ne, however, the expected effect was about 70%, much larger than the corrections.

For such large effects the second-order perturbation approximation is not applicable, and the deBoer-Winther program for multiple Coulomb excitation[2]) has been used for the analysis of the experimental data. Nevertheless, the perturbation approximation is useful for designing the experiments and to give a qualitative physical idea of the situation. Using this approximation, a measure of the magnitude of the reorientation effect is given by the ratio of the interference term to the first order term. For the excitation of the target:

$$r_T = \frac{A_p}{Z_T} \frac{\Delta E_T}{(1 + A_p/A_T)} \langle 2^+ || \mathcal{M}(E2) || 2^+ \rangle_T K(\theta,\xi) \quad , \qquad (1)$$

and for the excitation of the projectile:

$$r_P = \frac{A_p}{Z_p} \frac{\Delta E_P}{(1 + A_p/A_T)} \langle 2^+ || \mathcal{M}(E2) || 2^+ \rangle_P K(\theta,\xi) \quad , \qquad (2)$$

where, Z and A are the charge and mass numbers, ΔE is excitation energy, and the suffixes P and T correspond to the projectile and the target respectively. The static quadrupole moment is related to the reduced matrix element by:

$$eQ = -\frac{4}{5}\sqrt{\frac{2\pi}{7}} \langle 2^+ || \mathcal{M}(E2) || 2^+ \rangle \quad . \qquad (3)$$

The term $K(\theta,\xi)$ is a function which is sensitive to the scattering angle, θ but not very dependent on the beam energy. The advantage of using projectile excitation can be recognized from these formulae as being Z_T/Z_p.

In the usual experiments on target nuclei the effect has been observed by comparison of excitation probabilities for several values of the parameters, A_p and θ. For projectile excitation, however, eq. (2) shows that the scattering angle, θ, is the only parameter experimentally variable to measure the effect. The differential cross sections calculated by the deBoer-Winther program for a typical case are shown in fig. 1.

2. Experimental

The reorientation effects in the projectile excitation were observed by comparing the excitation probabilities at backward (160°) and at 90° scattering angles. A convenient way to measure the excitation probabilities of the projectile at the two different scattering angles was by comparing them with those of the target nucleus measured simultaneously. This method requires that the B(E2) values and the quadrupole moment in the target nucleus be known (or reliably estimated) to the required accuracy.

In this way, the efficiencies of the particle counters have been cancelled out except for small corrections. It was a further advantage of this method that the ratio of the excitation probability of the projectile to that of the target was less sensitive to the beam energy than the individual probabilities. The beam energy had an uncertainty of approximately two percent.

For all the target nuclei used, the reorientation effect in the target excitation was small compared with the effect in the projectile. The nuclei

^{120}Sn, ^{130}Te, and ^{148}Sm were used as targets for the measurements on ^{20}Ne, and ^{130}Te and ^{148}Sm were used for ^{22}Ne.

A schematic drawing of the experimental arrangement is shown in fig. 2. The beam of ^{20}Ne or ^{22}Ne was produced by the Berkeley Hilac and several different energies were used on each target nucleus in order to detect any interference due to nuclear reactions. The targets were about 1 mg/cm^2 thick.

The scattered particles were detected by a ring detector for back-scattered particles and by a circular detector at a scattering angle of 90°. The coincidence measurements were made between the two particle counters and a NaI(Tl) counter (5 cm × 5 cm or 7.5 cm × 7.5 cm) at 55° relative to the beam direction. In order to identify the particle signals from the two counters a time delay of about 160 ns was added to the signal from the 90° particle detector relative to the signal from the back-scatter detector. This produced two prompt peaks in the time spectrum. The energy signals from the two particle detectors were mixed together after the slow amplifiers; the gain of the amplifiers were adjusted so that there was no overlap of the spectra. The signals for the time spectra, particle spectra, and γ-ray spectra, and a counter identification signal were fed into a PDP-7 computer using a multiparameter program[3]).

A typical example of the experimental data obtained by off-line analysis is shown in fig. 3. The time resolution was between 15 and 30 ns depending on the experimental conditions for each run. To subtract the accidental coincidences, a window was set between the two prompt peaks in the time spectrum as shown in fig. 3a. Integration of the peaks in the sorted γ-ray spectra (fig. 3 d,e) produced (after subtraction of the accidental coincidences) the photo-peak areas N_P^{160}, N_T^{160}, N_P^{90}, and N_T^{90}, where the superscript denotes the scattering angle and the subscript distinguishes between the projectile, P, and target, T, nuclei.

From these four quantities the ratios of the excitation probability of the projectile to that of the target, R^{160} and R^{90}, and the double ratio $\mathcal{R}$ were calculated according to:

$$R^{160} = \left(\frac{N_P^{160}}{N_T^{160}}\right)\cdot\left(\frac{\varepsilon(E_\gamma^T)}{\varepsilon(E_\gamma^P)}\right) \quad , \tag{4}$$

$$R^{90} = \left(\frac{N_P^{90}}{N_T^{160}}\right)\cdot\left(\frac{\varepsilon(E_\gamma^T)}{\varepsilon(E_\gamma^P)}\right) \quad , \tag{5}$$

$$\mathcal{R} = \left(\frac{R^{160}}{R^{90}}\right) \quad , \tag{6}$$

where $\left(\frac{\varepsilon(E_\gamma^P)}{\varepsilon(E_\gamma^T)}\right)$ is the ratio of the photo-peak efficiencies of the NaI(Tl) counter for the γ-ray energy of the projectile nucleus to that of the target nucleus. Only two of these three ratios are independent, but the consistency among them is important in considering the magnitude of the experimental uncertainties. The double ratio $\mathcal{R}$ is less sensitive to the reorientation effect than is the single ratio, R^{160}; however, the double ratio is more important because to first order the B(E2; $0^+\rightarrow 2^+$) values of the target and projectile cancel out, as do the differences in the photo-peak efficiencies of the NaI(Tl) counter.

Typical results of the experiments are shown in fig. 4 and 5 together with 1) the calculated best-fit curves which will be discussed in the next section, and 2) the curves with no reorientation effect.

3. Analysis of Data

The experimental data were analyzed by comparison with the calculated results from the deBoer-Winther Coulomb excitation program[2]). To use this program for projectile excitation, the roles of the target and projectile were reversed, and the input and output data had to be treated accordingly. As mentioned previously, the large size of the reorientation effect in projectile excitation makes the experiment less sensitive to the many small corrections. However, the following effects, discussed below, were examined and, where necessary, corrections were made on the experimental data or the calculated results:

1) Effects due to nuclear reactions
2) Quantum mechanical effects
3) Finite solid angle of the particle counter
4) Finite solid angle of the γ-counter
5) Finite thickness of the target
6) Change of the γ-ray angular distribution and solid angle due to the motion of the γ-emitter
7) Change of the detection efficiency of the γ-ray due to the Doppler-shift
8) Attenuation of the γ-ray angular distribution due to the hfs field
9) Effects of other low-lying states
10) Effects of higher-order excitation

1) The energy of the incident beam was kept below the "safe energy"[1]), which corresponds to the Coulomb barrier height at 3 fermis out from the nuclear surface, $r_s = 1.25\ (A_p^{1/3} + A_T^{1/3}) + 3$ fermi. This "safe energy" has been questioned for some types of experiment[4]). In the present experiments this question was examined by lowering the incident energy to 80% of the safe energy (E_s) as

shown in figs. 4 and 5. The lack of significant deviations verified that the safe energy is indeed sufficiently low for the present experiment. Furthermore, a measurement has been made at an energy 10% higher than the safe energy, and still no significant deviation was observed (fig. 4a). It thus seems that the above safe energy is satisfactory for the present experiments.

2) Since the parameter $\eta = Z_P Z_T e^2/\hbar v$ for the present case is 40-50, the semiclassical approximation is expected to be well justified[5]).

3,4,5) A correction for the finite solid angles of the particle detectors has been made by numerical integration over the detector surface. The finite target thickness correction has also been made by numerical integration, and corrections for the finite solid angle of the γ detector have been made from the table of Q_2 and Q_4 given by Yates[6]).

6) Since the life-times of the 2+ states of the nuclei involved in the experiment were short, the simple geometrical correction due to the spatial deviation of the origin of γ emission from the target position was negligible (< 0.5 mm in the largest case of ^{22}Ne or ^{148}Sm). However, the effect of the moving origin was not negligible. For the γ-rays in coincidence with the back-scatter counter, the correction was calculated by integration of the formula for the angular distribution in the laboratory system[1]):

$$W(\theta_L)d\Omega = [1 + A_2P_2(\cos\theta_L) + A_4P_4(\cos\theta_L) + 2\frac{v}{c}\{(1 - \frac{1}{5}A_2)P_1(\cos\theta_L) + (\frac{6}{5}A_2 - \frac{2}{3}A_4)P_3(\cos\theta_L) + \frac{5}{3}A_4P_5(\cos\theta_L)\}]\,d\Omega \quad . \qquad (7)$$

This is derived from the formula,

$$W(\theta_N)d\Omega_N = [1 + A_2P_2(\cos\theta_N) + A_4P_4(\cos\theta_N)]d\Omega_N \quad , \qquad (8)$$

for the system fixed on the γ-emitting nucleus; but neglecting higher order terms in v/c. Fortunately, due to the angular distribution, the actual numerical value of this correction crossed zero for γ-angles around 55 degrees. For the γ-rays in coincidence with the 90° particle counter, the calculation of the correction is complicated and has been done numerically. Two different arrangements of the particle counter relative to the γ-counter were used to test this correction. The earlier one was a coplanar arrangement of γ- and particle counters, which required corrections up to 10% in the value of R^{90}. The other arrangement was the one shown in fig. 2, where the direction of γ-ray observation was perpendicular to the motion of the nuclei. But even in this case the corrections were still about 5%.

7) The correction for the change of detection efficiency of the γ rays due to the Doppler shift was approximately proportional to v/c and had a sign opposite to the previous correction. Thus it cancelled part of that correction and reduced the uncertainty due to estimation of the effective velocity.

8) Correction for the attenuation of the γ-ray angular distribution due to the hyperfine field effective in the recoiling ions[7]) is one of the most serious problems in heavy-ion reactions or Coulomb excitation. In the present case, the effect was examined in separate experiments. The attenuation factors, G_2 and G_4, have been determined by measuring the angular distribution of the γ-rays in coincidence with back-scattered particles. The measured values of G_2

were 0.94, 0.90, 0.98, 0.98, and 0.90 for the γ-rays of ^{20}Ne, ^{22}Ne, ^{130}Te, ^{120}Sn, and ^{148}Sm, respectively.

9,10) In the light nuclei the interference due to low-lying states is generally expected to be small. The estimation of the effects due to other states was made using a new version of the deBoer-Winther program which is able to calculate E1, E3, and E4 excitation, as well as mixed excitations; E2 + E4 and E1 + E3. The results are shown in Table 1 for the case of ^{20}Ne, and indicate that the effects are small. The effect of the 4+ state was calculated using the experimental ratios of $\frac{B(E2,\ 2^+ \rightarrow 4^+)}{B(E2\ \ 0^+ \rightarrow 2^+)}$ deduced from lifetime data[8]) and was taken into account in the analysis. Corrections were also made for E4 excitation to the 4+ state and E4 reorientation in the 2+ state, calculated using β_2 and β_4 from (p,p') experiment[9]). However, no correction has been made for the other effects. Nor has any correction been made for the simultaneous excitation of both target and projectile nuclei; estimates again indicate a small effect ($< 2\%$). But, uncertainties of ±5 percent were introduced into the final results to allow for these uncorrected effects.

4. Results

After corrections, the best theoretical fits to the experimental points were found by least-square fitting to the experimental sets of three numbers, R^{160}, R^{90}, and $\mathcal{R} = (R^{160}/R^{90})$ using correlated weight functions. For convenience of calculation, the intrinsic quadrupole moment Q_0 for the $0^+ \rightarrow 2^+$ transition and the ratio (Q/Q_{rot}) were used as the parameters to be determined, where Q is the static quadrupole moment of the 2+ state (eq. (3)) and Q_{rot} is the value for Q calculated from Q_0 using the rigid rotor model:

$$e^2Q_0^2 = \frac{16\pi}{5} B(E2,\ 0^+ \rightarrow 2^+) \quad , \tag{9}$$

$$Q_{rot} = -\frac{2}{7} Q_0 \quad . \qquad (10)$$

The results of the parameter search are summarized in Tables 2 and 3.

Since the excitation probability of Ne at each angle has been measured relative to the target excitation probability, the final results depend on the B(E2) values and static moments of the target nuclei. The uncertainty in the results comes mainly from these factors. The best target for the ^{20}Ne experiment was ^{120}Sn. The excitation probability was comparable to that of ^{20}Ne and the B(E2) value has been determined[10]) with an accuracy of 5%. No data on the static quadrupole moment of the 2+ state were available; however, it seems likely that the reorientation effect in ^{120}Sn is small. Tha analysis was made by assuming: $Q(^{120}Sn) = 0.0 \pm 0.5\ Q_{rot}(^{120}Sn)$. The effect of the excitation of higher states in ^{120}Sn has been estimated to be negligible. The results of the recent measurement[11]) of the static quadrupole moment of the 2+ state and the $B(E2, 0^+ \rightarrow 2^+)$ value in ^{130}Te have been used in the present analysis. The value of $B(E2, 0^+ \rightarrow 2^+)$ is indeed just the mean value of earlier experiments[12,13]). There are several results for the value of the $B(E2, 0^+ \rightarrow 2^+)$ in ^{148}Sm by Coulomb excitation which do not agree with each other. However, the measurement of the lifetime of the 2+ state has recently been done by the "recoil distance method"[14]), which is much simpler and therefore a less ambiguous method. The B(E2) value deduced from this lifetime was used for the present analysis. The static quadrupole moment[15,16]) of the 2+ state in ^{148}Sm and the E2 and E3 excitation probabilities for the higher 2+ and 3- states[17]) have been measured with sufficient accuracy for the present analysis.

5. Discussion

From the values of Q_0 obtained, the values of $B(E2, 0^+ \rightarrow 2^+)$ for ^{20}Ne and ^{22}Ne have been calculated and compared with previous results in Table 4. For both ^{20}Ne and ^{22}Ne, the present values agree with previous Coulomb excitation experiments, but are somewhat larger than the average values deduced from lifetime measurements. The main uncertainties in the present $B(E2, 0^+ \rightarrow 2^+)$ values come from the errors in the B(E2) values of the target nuclei and from the uncertainty in the incident beam energy. On the other hand, it was found that the value of Q obtained is less sensitive to these factors, because Q is determined mainly from the ratio of the excitation probabilities at 90° and 160° ($\mathcal{R}$), whereas the B(E2) value comes directly from the probabilities relative to those of the target (R^{160} and R^{90}).

The values obtained for the static quadrupole moments of the first excited state of ^{20}Ne and ^{22}Ne are:

$$Q(^{20}Ne) = -0.24 \pm 0.03 \text{ barns and}$$

$$Q(^{22}Ne) = -0.21 \pm 0.04 \text{ barns.}$$

These results agree with the value given in a paper ($Q(^{20}Ne) = -0.27 \pm .11$ b, $Q(^{22}Ne) = -0.21 \pm .06$ b)[18] which came out during the analysis of the present experiment. In both cases of ^{20}Ne and ^{22}Ne, Q is about 30% larger than Q_{rot}. In still another light nucleus, ^{24}Mg, the static quadrupole moment of the first excited state is also about 30% larger than that calculated for Q_{rot}[19]. It is significant that three different experimental methods all give values for Q which are larger than Q_{rot}. These methods presumably depend in different ways on any effects which

were not explicitly taken into account. In addition, the present method involves a very large reorientation effect ($\sim$ 70%) and thus should be less sensitive to any other effects. It thus seems that these quadrupole moments are, indeed, larger than the rotational values.

In Table 5, E2 reduced matrix elements of ^{20}Ne and ^{22}Ne for which data are available from the literature have been calculated and compared with values given by the rigid-rotor model. Contrary to the diagonal elements, the higher non-diagonal elements appear to be smaller than the rigid-rotor values. This effectively disposes of the idea that the larger static moment could be due to simple stretching of the deformed rotating nucleus. Perhaps this rather suggests that the wave functions of the different levels do not have exactly the same intrinsic structure. Due to the poorer overlap of the different wave functions, the off-diagonal matrix elements are then reduced relative to the diagonal elements. Hartree-Fock or shell-model calculations can produce static moments as large as the rotational value, but no calculations exist which yield values larger than the rotational value. For example, a shell model calculation by Akiyama et al.[20] with a phenomenological effective interaction produced the value -0.19 barns for the quadrupole moment of ^{20}Ne with an effective charge normalized to the B(E2; $0^+ \rightarrow 2^+$) value. This value is close to Q_{rot} and so about 30% smaller than the experimental values.

It is not really surprising that the rigid-rotor model is not strictly applicable for these light s-d shell nuclei, because of the small number of nucleons involved. It is perhaps, more important to point out that these data rather show the general applicability of this model. The energies of the levels provide additional support for the model. It will be interesting to measure the static moments of some additional nuclei in this region, and projectile excitation appears to be a most promising method.

Acknowledgment

We should like to express our appreciation to Dr. R. Nordhagen for his interest and valuable discussions. We are indebted to the Hilac crew for their help, especially in producing the stable Ne beams with high duty cycle ($\sim$ 20%) which were indispensable for the coincidence experiments. We would like to thank Mr. D. Landis for his help with the electronics, Mr. R. Lothrop for providing the particle detectors, and Mr. T. Gee for making the targets. One of us (K.N.) is grateful to Professor I. Perlman for the opportunity to participate in this experiment at the Lawrence Radiation Laboratory.

References

1) J. deBoer and J. Eichler, "The Reorientation Effect", in Advance in Nuclear Physics Vol. 1 (Academic Press, N. Y., 1968).

2) A. Winther and J. deBoer, in Coulomb Excitation, a collection of reprints (Academic Press, N.Y., 1966) p. 303.

3) Program prepared by L. Robinson.

4) D. Cline, H. S. Gertzman, H. E. Gove, P. M. S. Lesser and J. J. Schwartz, to be published.

5) K. Alder and H. K. A. Pauli, Nucl. Phys. A128 (1969) 193.

6) M. J. L. Yates, in Alpha, Beta and Gamma-Ray Spectroscopy, ed. by K. Siegbahn (North Holland Publishing Co., Amsterdam, 1965) 1691.

7) I. Ben Zvi, P. Gilad, M. Goldberg, G. Goldring, A. Schwartzschild, A. Sprinzak and Z. Vager, Nucl. Phys A121 (1968) 592.

8) S. J. Skorka, J. Hertel and T. W. Retz-Schmidt, Nucl. Data Vol. 2, p. 347; J. H. Anderson and R. C. Ritter, Nucl. Phys. A128 (1969) 305.

9) R. de Swiniarski, C. Glashausser, D. L. Hendrie, J. Sherman, A. D. Baccher and E. A. MacClatchie, Phys. Rev. Letters 23 (1969) 317.

10) P. H. Stelson, F. K. McGowan, R. L. Robinson, W. T. Milner and R. O. Sayer, Phys. Rev. 170 (1968) 1172.

11) A. Christy, I. Hall, R. P. Harper, I. M. Nagib and B. Wakefield, Contribution to the International Conference on Properties of Nuclear States, Montreal, (1969).

12) P. H. Stelson and F. K. McGowan, Phys. Rev. 110 (1958) 489.

13) G. M. Temmer and N. P. Heydenburg, Phys. Rev. 104 (1956) 967.

14) R. M. Diamond, F. S. Stephens, K. Nakai and R. Nordhagen, to be published.

15) H. S. Gertzman, D. Cline, H. E. Gove, P. M. S. Lesser and J. J. Schwartz, Bull. Am. Phys. Soc. 13 (1968) 1471.

16) J. J. Simpson, D. Eccleshall, M. J. L. Yates and N. J. Freeman, Nucl. Phys. A94 (1967) 177.

17) R. J. Keddy, Y. Yoshizawa, B. Elbek, B. Herskind and M. C. Olesen, Nucl. Phys. A113 (1968) 676.

18) D. Schwalm and P. Povh, Phys. Letters 29B (1969) 103.

19) O. Hausser, B. W. Hooton, D. Pelte, T. K. Alexander and H. C. Evans, Phys. Rev. Letters 22 (1969) 359.

20) A. Akiyama, A. Arima and T. Sebe, Nucl. Phys. A138 (1969) 273.

Table 1. Effects of the higher states and higher order processes on $Q(^{20}Ne)$.

	State			% Effect on			Corrected?
	E (MeV)	I^π		Yield of 2^+ state 160°	90°	Q	
Effect of 4^+ state	4.25	4^+	$\frac{B(E2,\ 2^+ \rightarrow 4^+)}{B(E2,\ 0^+ \rightarrow 2^+)} = 1.62 \pm 0.4$ [a]	+2.0	+0.6	+2%	yes
Effect of E4 moment							
a) E4 excitation	4.25	4^+	$Q_4 = +0.024\ eb^2$ [b]	-2.2	-0.7	-2%	yes
b) E4 reorientation effect	1.63	2^+					
Reorientation effect in 4^+ state	4.25	4^+	$Q(4^+) = Q_r(4^+)$ [c]	0.2	0.	$< 1\%$	no
Effect of $2^{+\prime}$ state	7.43	2^+	$B(E2,\ 0^+ \rightarrow 2^+) = 10B_{sp}$ [c]	2.7	1.3	$\lesssim 2\%$	no
Effect of 3^- state	5.62	3^-	$B(E3,\ 0^+ \rightarrow 3^-) = 10B_{sp}$ [c]	0.1	0.4	$< 1\%$	no

[a] Reference 8.

[b] Reference 9.

[c] Assumptions: $Q_r(4+)$ is a value calculated from $B(E2,\ 0^+ \rightarrow 2^+)$ by the rigid rotor model. $B_{sp}\ (E\lambda)$ is the single particle value.

UCRL-18959

Table 2. Summary of the experimental results for ^{20}Ne.

Target	Basis of calculation: B(E2;↑ target) (e^2b^2)	Basis of calculation: Q(target) (b)	Results of least square fitting: Q_0 (b)	Results of least square fitting: Q/Q_{rot}	B(E2,↑ ^{20}Ne) (e^2b^2)	Q(^{20}Ne) (b)
^{120}Sn	0.23±0.012[a]	$+0.5\|Q_r\|$	0.69±0.04	1.11±0.08	0.048±0.0055	-0.22±0.02
		0.0	0.69±0.04	1.26±0.085	0.048±0.0055	-0.25±0.02
		$-0.5\|Q_r\|$	0.69±0.04	1.40±0.09	0.048±0.0055	-0.28±0.02
	0.23±0.012[a]	$(0\pm0.5)\|Q_r\|$[b]	0.69±0.04	1.26±0.17	0.048±0.0055	-0.25±0.036
^{130}Te	0.30±0.03[c]	-0.15±0.2[c]	0.69±0.065	1.20±0.18	0.048±0.009	-0.24±0.035
^{148}Sm	0.79±0.07[d]	-0.5± 0.3[e]	0.69±0.061	1.19±0.15	0.048±0.0086	-0.23±0.035
Summary				1.20±0.15*	0.048±0.007*	-0.24±0.03*

*Possible systematic errors of (±5%) have been included.

[a]Reference 10.

[b]Assumption: Q_r is a value calculated from B(E2, $0^+ \rightarrow 2^+$) using the rigid rotor model.

[c]Reference 11.

[d]Reference 14.

[e]Reference 15, 16.

UCRL-18959

Table 3. Summary of the experimental results for ^{22}Ne.

Target	Basis of calculation		Results of least square fitting			
	B(E2;↑ target) (e^2b^2)	Q(target) (b)	Q_0 (b)	Q/Q_{rot}	B(E2;↑ ^{22}Ne) (e^2b^2)	Q(^{22}Ne) (b)
^{130}Te	0.30±0.03[c]	-0.15±0.2[c]	0.56±0.06	1.33±0.23	0.031±0.007	-0.21±0.045
^{148}Sm	0.79±0.07[d]	-0.5 ±0.3[e]	0.57±0.06	1.23±0.17	0.034±0.007	-0.205±0.03
Summary				1.28±0.20*	0.033±0.006*	-0.21±0.04*

*Possible systematic errors of (±5%) have been included.

[a-e]See footnotes for Table 2.

UCRL-18959

Table 4. Comparison of the $B(E2,0^+ \rightarrow 2^+)$ values from various experiments.

Reference	$B(E2,0^+ \rightarrow 2^+)$ (e^2b^2)	Weight[a] for average	Method[b]
^{20}Ne			
Present	0.048 ± 0.007	2	CE
AN 69	$0.026^{+0.005}_{-0.010}$	2	DA
GR 69	0.042 ± 0.010	2	DA
EV 65	0.029 ± 0.003	4	DA
CL 61	$0.063^{+0.014}_{-0.032}$	1	DA
AN 60	0.047 ± 0.020	1	CE
DE 56	0.046 ± 0.020	1	DA
Average	0.039 ± 0.004		

(continued)

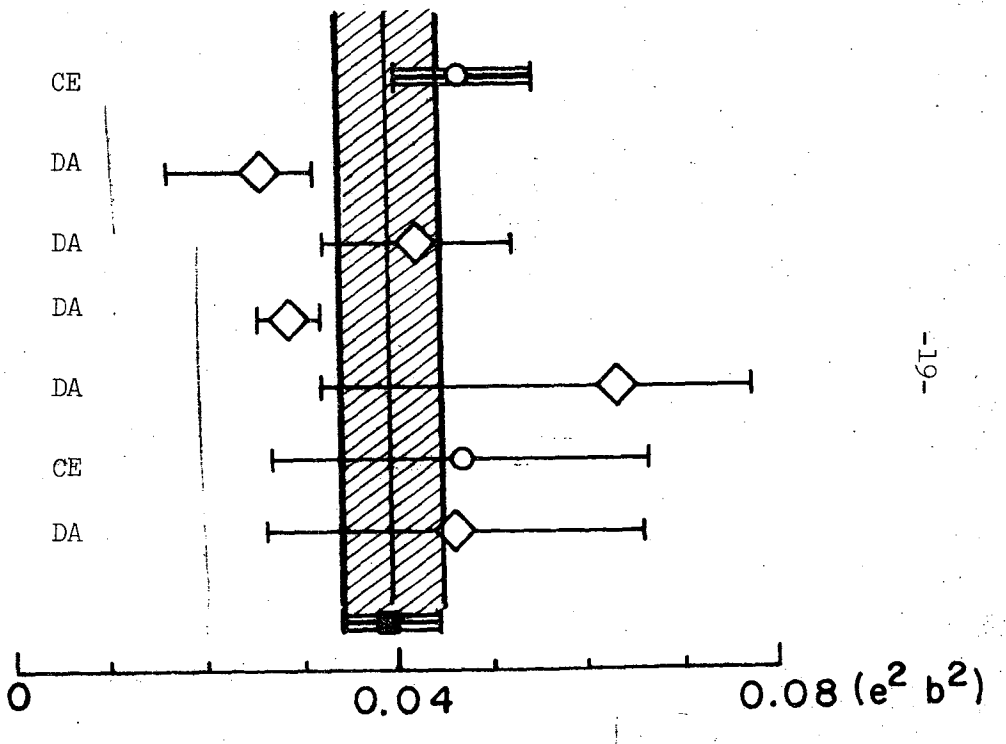

XBL697-3353

Table 4. continued

Reference	$B(E2,0^+\rightarrow 2^+)$ (e^2b^2)	Weight[a] for average	Method[b]
^{22}Ne			
Present	0.033±0.006	2	CE
JO 69	0.026±0.003	4	RD
LI 66	0.015±0.006	2	DA
ES 64	0.019±0.011	1	DA
AN 60	0.039±0.014	1	CE
Average	0.026±0.003		

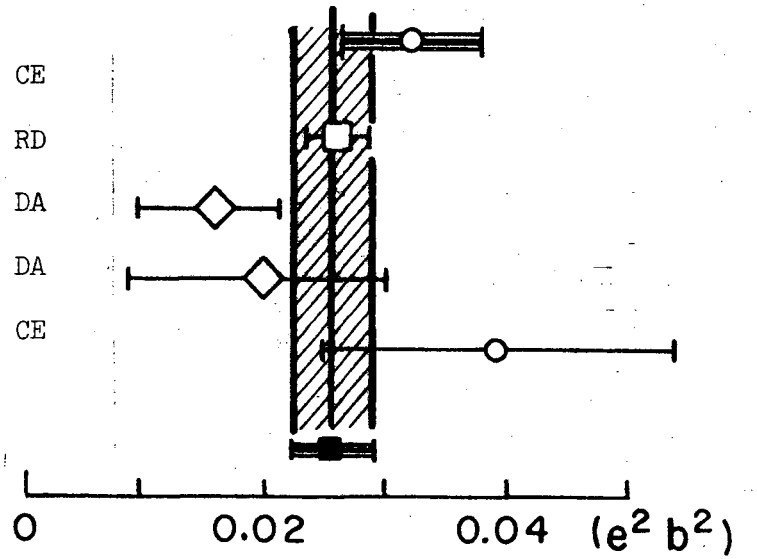

XBL697-3354

[a]Rounded values of reciprocals of the errors.

[b]CE; Coulomb Excitation, DA; Doppler-Shift Attenuation Method, RD; Recoil Distance Method.

[c]References:

AN 69 - J. H. Anderson et al., Nucl Phys. A128 (1969) 305;

GR 69 - H. Grawe et al., Nucl. Phys. A127 (1969) 13;

EV 65 - H. C. Evans et al., Can. J. Phys. 43 (1965) 82;

CL 61 - M. A. Clark et al., Can. J. Phys. 39 (1961) 1241;

(continued)

Table 4. continued

AN 60 - D. S. Andreyev et al., Nucl Phys. 19 (1960) 400;

DE 56 - S. Devons et al., Proc. Phys. Soc. A69 (1956) 173;

JO 69 - K. W. Jones et al., Phys. Rev. 178 (1969) 1773;

LI 66 - K. P. Lieb, Verhandl. DPG (4) 1 (1966) 38;

ES 64 - M. A. Eswaran et al., Can. J. Phys. 42 (1964) 1311.

Table 5. Comparison of reduced matrix elements.

(a) ^{20}Ne

Experimental Data	$B(E2,0^+ \rightarrow 2^+)$	Q	$B(E2,2^+ \rightarrow 4^+)$	$B(E2,4^+ \rightarrow 6^+)$
	$0.039\pm0.004(e^2b^2)^a$	$-0.24\pm0.03(b)^b$	$0.0094\pm0.0016(e^2b^2)^c$	$0.013\pm0.003(e^2b^2)^c$
	$\langle 2\|\mathcal{M}\|0 \rangle$	$\langle 2\|\mathcal{M}\|2 \rangle$	$\langle 4\|\mathcal{M}\|2 \rangle$	$\langle 6\|\mathcal{M}\|4 \rangle$
$\langle f\|\mathcal{M}\|i \rangle$	0.198 ± 0.010	0.316 ± 0.040	0.216 ± 0.019	0.343 ± 0.040
$\langle f\|\mathcal{M}\|i \rangle$	$(1.0)^a$	1.33 ± 0.18	0.68 ± 0.07	0.85 ± 0.011
$\overline{\langle f\|\mathcal{M}\|i \rangle}_{rot}$		(1.22 ± 0.15^d)	(0.78 ± 0.2^e)	

(b) ^{22}Ne

Experimental Data	$B(E2,0^+ \rightarrow 2^+)$	Q	$B(E2,2^+ \rightarrow 4^+)$
	$0.026\pm0.003(e^2b^2)^a$	$-0.21\pm0.04(b)^b$	$0.0097\pm0.0022(e^2b^2)^c$
	$\langle 2\|\mathcal{M}\|0 \rangle$	$\langle 2\|\mathcal{M}\|2 \rangle$	$\langle 4\|\mathcal{M}\|2 \rangle$
$\langle f\|\mathcal{M}\|i \rangle$	0.162 ± 0.010	0.276 ± 0.053	0.22 ± 0.025
$\langle f\|\mathcal{M}\|i \rangle$	$(1.0)^a$	1.43 ± 0.29	0.85 ± 0.11
$\overline{\langle f\|\mathcal{M}\|i \rangle}_{rot}$		(1.28 ± 0.20^d)	

[a] Table 4. The rotational values of matrix elements $\langle f\|\mathcal{M}\|i \rangle$ are calculated using the average $B(E2,0^+ \rightarrow 2^+)$ values in Table 4.

[b] Present results.

[c] Reference 8.

[d] Internal value in the present measurement (Table 2 and 3).

[e] Internal value in Reference AN 69 in Table IV.

UCRL-18959

Figure Captions

Fig. 1. Calculated differential cross sections for Coulomb excitation of the projectile and the target for a typical case of 56 MeV ^{20}Ne on ^{120}Sn. The cross sections are calculated for Q = 0 and Q = $\pm Q_r$; Q_r is the value calculated from B(E2, $0^+ \rightarrow 2^+$) using the rigid-rotor model.

Fig. 2. Experimental arrangement and circuit diagram. SSD, Solid State Detector; FA, Fast Amplifier; PS, Pulse Shaper; MIX, Mixer; TAC, Time to Amplitude Convertor; LA, Linear Amplifier; HRA, High Rate Amplifier; PUR, Pile Up Rejector; LG, Linear Gate; MA, Mixer Amplifier.

Fig. 3. Typical data from the multidimensional analysis; a) Time spectrum (gated by γ-ray signals whose energies were higher than 300 keV), b) Particle spectrum, c) Total γ-ray spectrum, d) e) f) Gated γ-ray spectra by the windows shown in a) and b).

Fig. 4. Typical results of the experiments and least-square fittings on ^{20}Ne. The solid lines show the best fit curves for the experimental points, and the dashed lines show the curves with Q(^{20}Ne) = 0. The data in (a) shown by open circles (at 70 MeV) are higher than the "safe energy" and were not included in the least square fitting. However they still fall on the best-fit curves (see discussion in § 3).

Fig. 5. Typical results of the experiments and least-square fittings on ^{22}Ne. The solid lines show the best fit curves for the experimental points, and the dashed lines show the curves with Q(^{22}Ne) = 0. The safe energy is indicated by E_s.

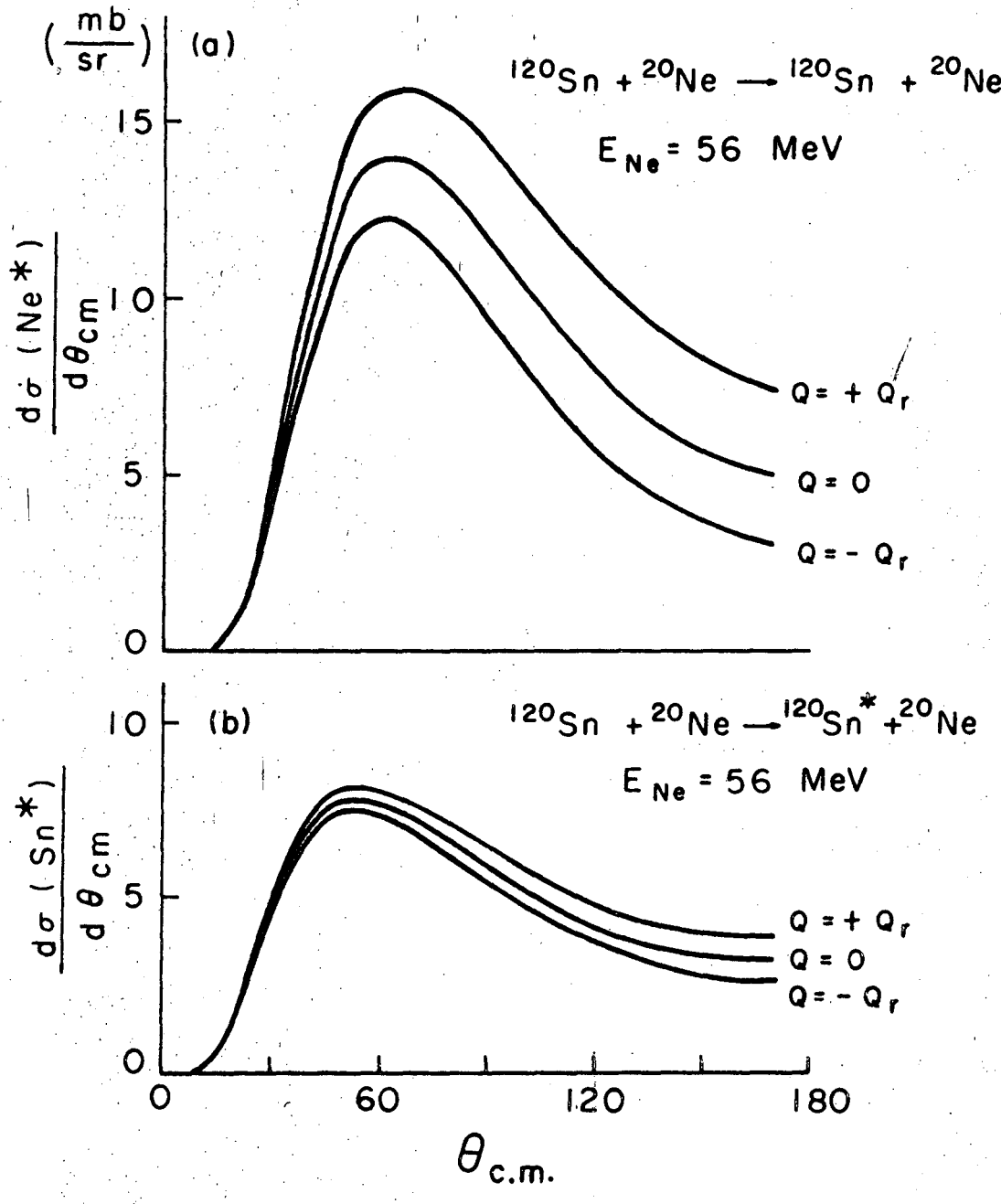

XBL697-3358

Fig. 1

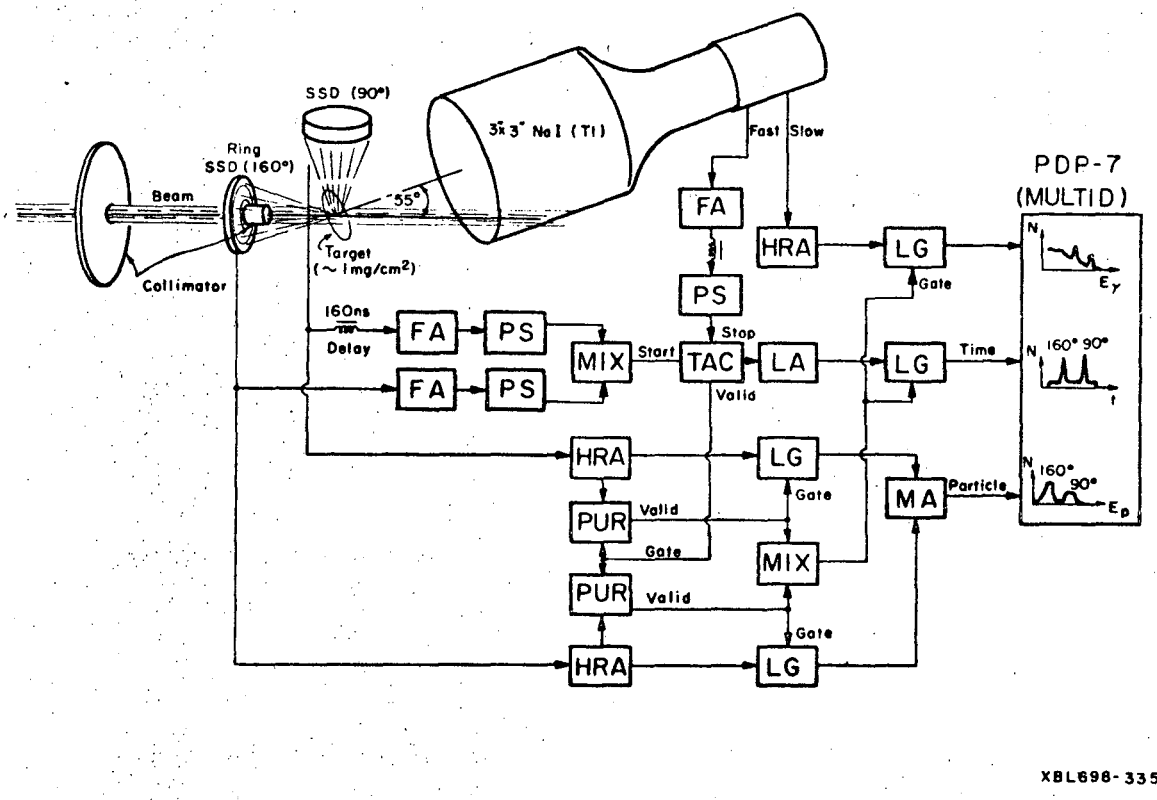
SSD (90°)
3"x3" NaI (Tl)
Fast
Slow
PDP-7
(MULTID)
Ring
SSD (160°)
Beam
55°
Target
(~ 1mg/cm²)
Collimator
FA
HRA
LG
Gate
PS
160ns
Delay
FA
PS
MIX
Start
Stop
TAC
LA
LG
Time
Valid
FA
PS
HRA
LG
Gate
PUR
Valid
MA
Particle
Gate
MIX
PUR
Valid
Gate
HRA
LG
N
Eγ
160° 90°
t
160°
90°
Ep
XBL698-3357

Fig. 2

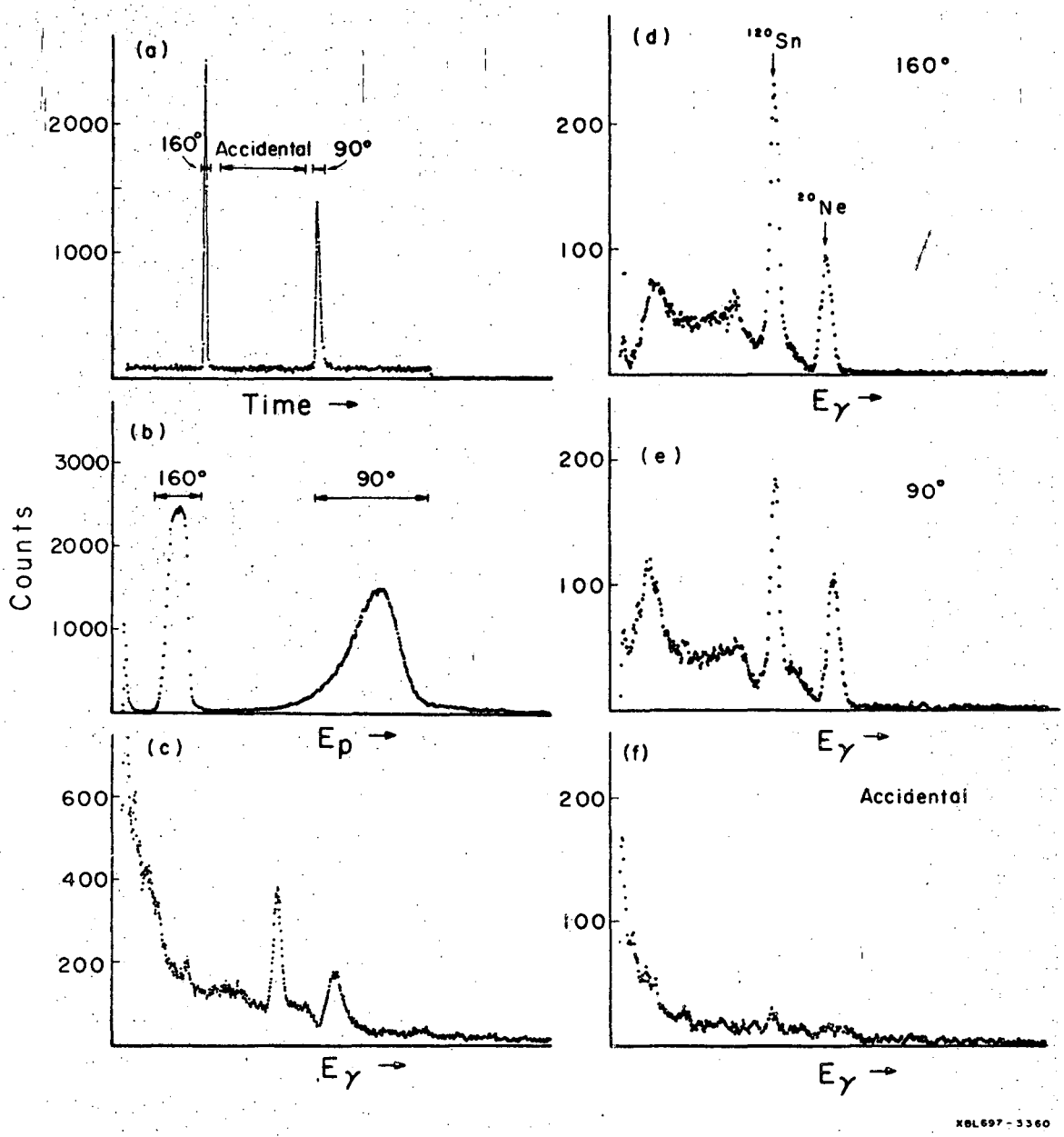
(a)
2000
1000
160°
Accidental
90°
Time →
(b)
3000
2000
1000
160°
90°
Counts
Ep →
(c)
600
400
200
Eγ →
(d)
120Sn
160°
200
100
20Ne
Eγ →
(e)
200
100
90°
Eγ →
(f)
200
100
Accidental
Eγ →
XBL697-3360

Fig. 3

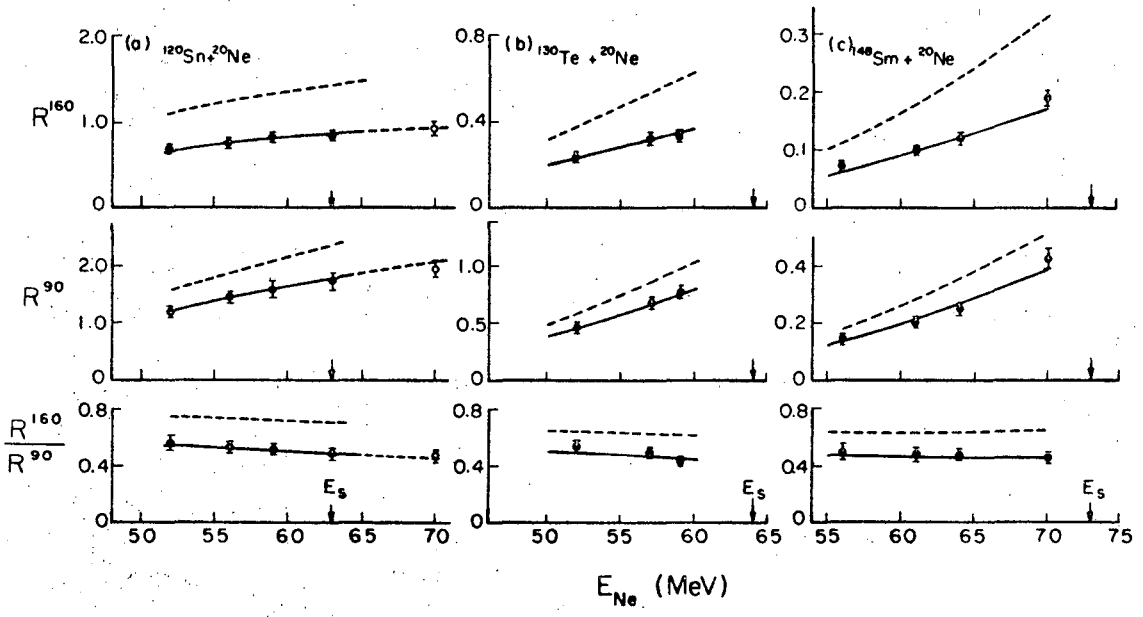
(a) $^{120}Sn + ^{20}Ne$
(b) $^{130}Te + ^{20}Ne$
(c) $^{148}Sm + ^{20}Ne$
R^{160}
R^{90}
$\frac{R^{160}}{R^{90}}$
E_s
E_{Ne} (MeV)
XBL697-3359

Fig. 4

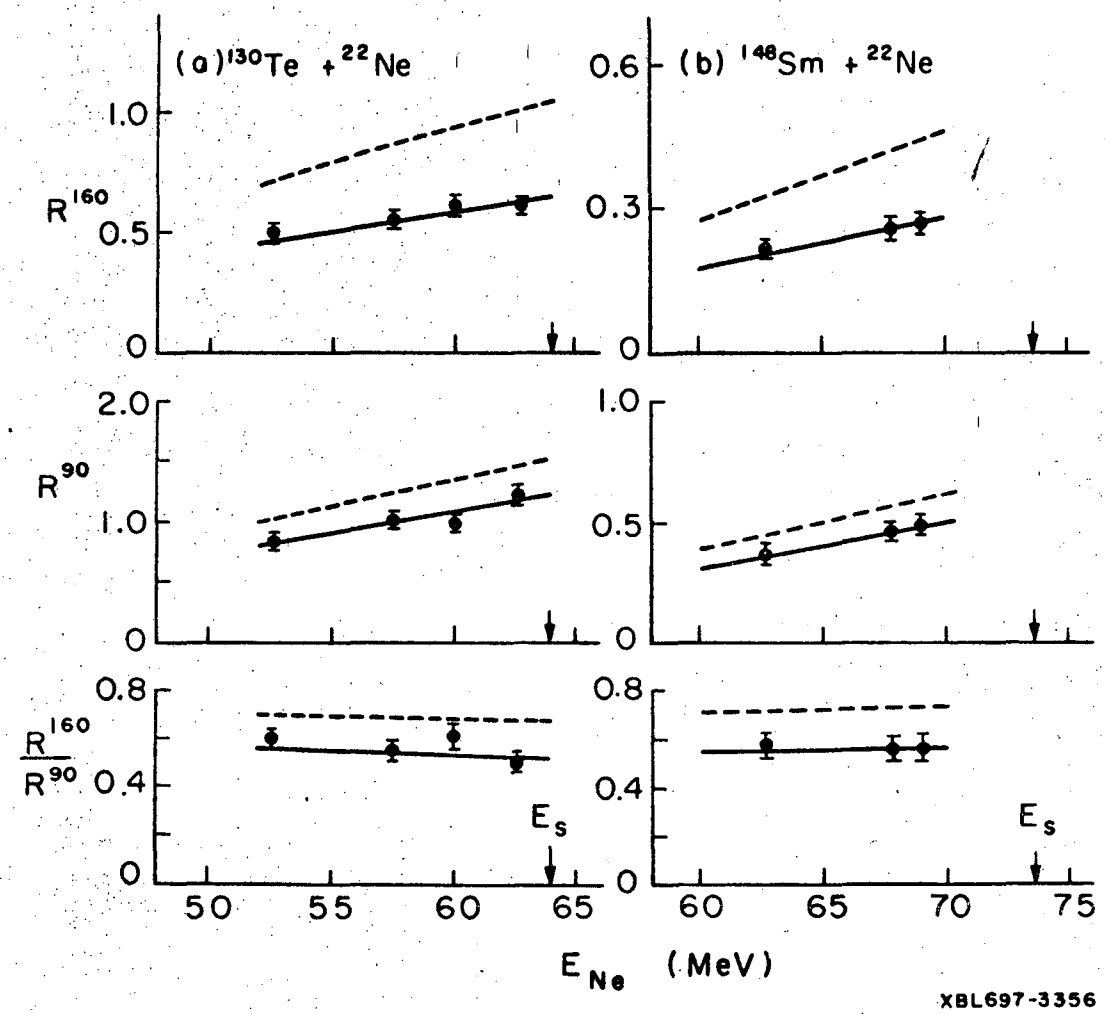
(a) ^{130}Te + ^{22}Ne
(b) ^{148}Sm + ^{22}Ne
R^{160}
R^{90}
$\frac{R^{160}}{R^{90}}$
E_s
E_{Ne} (MeV)
XBL697-3356

Fig. 5

TECHNICAL INFORMATION DIVISION
LAWRENCE RADIATION LABORATORY
UNIVERSITY OF CALIFORNIA
BERKELEY, CALIFORNIA 94720